

Supporting Information

Williams et al. 10.1073/pnas.0914211107

SI Text

Additional Background

Thus far, recent tree mortality and forest die-off events due to climatic disturbance have primarily been observed in case studies focusing on particular species and regions of interest (e.g., refs. 1–3). Assessments encompassing a broader range of forests have been limited because the temporal and spatial coverage of forest-growth data are insufficient (but see refs. 4 and 5). This problem may eventually be overcome in the US, in part by the USDA Forest Inventory and Analysis program that now collects a vast amount of forest-growth data annually throughout the country. Also holding promise are studies that use satellite imagery to monitor growth dynamics across large geographic areas (6–8). Like forest inventory data, however, satellite records are at present relatively short, and there are challenges in identifying and interpreting tree mortality from satellite data (e.g., compare the divergent findings of refs. 9–11).

Conveniently, many trees have been growing for hundreds or even thousands of years while annually recording environmental changes and tree growth rates in the form of their growth rings found in the cross-sections of their trunks. In general, wide rings are produced during years of optimal climatic conditions while thinner rings grow in response to poor conditions (12, 13). Statistically and mechanistically quantifiable relationships between ring widths and climate have provided a basis for using tree-ring width chronologies for reconstructing numerous past climate histories. Tree-ring scientists have collected cores and cross-sections from many thousands of trees and measured time series of tree-ring widths for thousands of sites around the world. A large database of annual tree-ring widths and standardizing ring-width index chronologies are archived in the International Tree-Ring Data Bank (ITRDB and maintained by the National Climate Data Center (NCDC) (see www.ncdc.noaa.gov/paleo/treering.html).

Although tree-ring width chronologies have most commonly been used to provide long-term “proxy” estimates of regional and broader-scale climatic variations, they have infrequently been used to estimate forest growth variations. A problem with using existing tree-ring width chronologies originally developed for climatic studies to evaluate forest growth is that the sites and trees within them were usually systematically selected and sampled for maximum climatic responsiveness, and not for obtaining an unbiased representation of forest populations or the spatial/geographic distributions of forests. At least two studies that we are aware of, however, have demonstrated that widely distributed (spatially) tree-ring width chronologies from relatively small numbers of sampled trees per site (stand) can provide useful representations of forest growth at the stand to regional scales. The two examples are from studies in southern Finland and SW US where ring-width records were directly compared with complete or statistically unbiased growth-inventory data representing many thousands of trees and large areas (14, 15).

Several other studies to date have attempted to infer forest growth responses to climate variability from ring-width chronologies. For example, Peterson and associates have collected and analyzed tree-ring data from many sites to determine the primary climate variables that affected annual growth rates for various species across a number of climate regimes within the montane Pacific Northwest (16–20). McKenzie et al. (21) analyzed 185 tree-ring records in search of positive growth trends since 1850 in western North America. They found that although annual growth rates had not significantly increased at the ma-

majority of sites, pronounced increases had occurred at some high-elevation and high-latitude sites. Although this conclusion is subject to the same concerns described above (nonrandom selection of the original sites and trees), no other dataset containing annual tree growth information across such a broad geographical, temporal, or taxonomic range is available. In this light, the McKenzie et al. (21) study represented an inspiring use of a multicentennial dataset of tree growth to evaluate an important ecological response to global climate change.

The tree-ring component of our study builds on these previous studies that have implicitly or explicitly inferred forest growth across geographic regions, species, and climate types from ring-width chronologies. It would certainly be valuable to carry out detailed assessments of the strengths and weaknesses of existing ring-width chronology data sets for estimating forest growth at various spatial scales. For example, it should someday be possible to compare tree-ring chronologies with incipient long-term inventory data sets (e.g., experimental forests, FIA plots etc.) at stand to regional scales.

Methods of Tree-Ring Analysis. Tree-ring data. We obtained 1,148 chronologies of tree-ring width index values for all sites within the continental United States listed by the ITRDB in September 2009, as well as four unpublished chronologies provided by the authors and H. Grissino-Mayer. Each chronology represents the average of multiple trees at a site (typically >10 trees). As opposed to raw ring widths, ring-width index (RWI) values were used for each site because they have been standardized to preserve interannual variability and remove long-term growth trends caused by aging and increasing trunk diameter (22). Removal of these long-term biological trends typically increases the proportion of interannual variability in ring-width values that can be explained by climate. Although RWI values cannot translate directly to estimates of productivity or growth rate in absolute terms (e.g., wood volume or whole-tree biomass increment per year), they generally represent relative radial growth rates fluctuating around a common mean index value of 1.0. A RWI value of 2.0 represents a year when radial growth was twice that of a normal year. A RWI of 0.5 represents a year when radial growth was half that of a normal year. We used the existing standardized index chronologies in the ITRDB that were provided by the contributors. Although the specific standardization approach (i.e., types of curves fitted to ring-width series, and various averaging and other time series treatments) varied among the chronologies, in general, the chronologies were developed to preserve most of the interannual to decadal variance that was in common among sampled trees within sites. See “The use of pre-standardized ring-width index records” in *SI Text* for more on this issue.

To increase the probability that each RWI record was not unduly influenced by anomalous individual trees, but instead represented the productivity of numerous trees, we only considered RWI values that were calculated using five or more tree cores. Notably, the ITRDB only clarifies how many cores, not trees, are represented in each chronology, but commonly, two cores are collected from each tree. We only considered chronologies with at least 60 annual RWI values (years) after 1895 so that we could evaluate statistical relationships between ring-width indices and a seasonal climate dataset that began in fall 1895. Ring-width records fit these criteria at 1,097 sites.

Notably, most RWI records used in this study were collected in the 1980s and 1990s and do not extend through much of the recent warming event that began in the mid-1970s. Seventy-three records

extend through 1979, 35% extend through 1989, and only 9% extend through 1999. This means that the majority of RWI records cannot reflect potentially long-term nonlinear growth responses to the warming trend of the most recent decades, such as adaptation or substantially decreased growth rates beyond some temperature threshold. All RWI records do, however, overlap with the warming trend that occurred between the 1910s and 1940s. The 1910s–1940s warming trend was comparable in magnitude and duration to the recent warming trend, allowing RWI records to more accurately represent long-term relationships between tree growth and temperature variability than they would have in the absence of a multidecadal trend. Notably, the past warming trend is not a perfect analog to the current trend because temperatures were generally cooler in the first half of the 20th century. Also, within the SW region, precipitation was relatively stable about the long-term mean during the 1910s through 1940s period. SW precipitation has declined from above the mean to below the mean during the recent warming event, likely exacerbating drought stress caused by increased temperatures (Fig. S1). See *SI Text* on growth models for a further discussion of nonlinear growth response to climate.

Climate data. We obtained monthly gridded climate data (total precipitation and average daily maximum, minimum, and dew point temperature) for 1895 through 2008 from the PRISM group at Oregon State University. PRISM datasets are grids with 2.5-arcminute (≈ 4 km) spatial resolution. For each tree-ring site, we averaged the records of the 9 grid cells (3 by 3) centered on the reported site because the locations of the sites were not always precisely reported. Using each site's monthly record of the four climate variables listed above, we calculated annual total precipitation, average daily minimum temperature, average daily maximum temperature, and average relative humidity for each 3-mo season, beginning with October through December and ending with July through September.

Notably, increasing concentrations of atmospheric carbon dioxide (CO_2) will likely have important impacts on plants, and these effects are anticipated to vary widely by region and species (23). The effect of CO_2 enrichment on tree growth is difficult to identify in RWI records, however, because the concentration of atmospheric CO_2 has been steadily rising throughout the industrial era without substantial interannual variability. Therefore, the decreasing radial growth rate that generally occurs in growing trees may mask a positive growth relationship with CO_2 . The naturally negative trend in ring-widths may also cause a negative growth relationship with increasing CO_2 to be difficult to interpret. The statistical standardization process used to eliminate ring-width trends associated with increasing tree-size are likely to remove any long-term growth trends associated with increased atmospheric CO_2 . We therefore made no specific effort to include the effects of the increasing atmospheric CO_2 on tree growth.

Growth model. Treating each of the 1,097 RWI records independently, we used multiple linear regression analysis to create a climate-based growth model for each tree population. Often, growth is most responsive to a given climate parameter (precipitation, maximum temperature, minimum temperature, and relative humidity) during a portion of the year, and depending on the time of year, the growth response may be positive or negative. We therefore evaluated the effect of each climate parameter during each of the four 3-mo seasons over a 12-mo period that begins in October and ends in September (4 climate parameters \times 4 seasons = 16 variables).

To reduce the probability of using climate variables that are statistically associated with, but do not actually impact tree growth, we only incorporated a given climate variable in a growth model if it made a "substantial contribution" to the predictability of ring-width indices. To do this, we conducted a forward step-wise regression. For each model, we began with the single variable that most strongly correlated with the RWI record. Using

this first variable, we initially developed a simple univariate linear model to predict RWI values. We established the strength of the initial model by calculating the coefficient of determination (R^2) between predicted and actual RWI values. Next, we independently tested each variable as a second potential predictor of RWI in a bivariate linear model. We chose the single variable that contributed to the greatest improvement in the model R^2 , and if R^2 improved by >0.02 , we accepted the new variable as a second RWI predictor. We repeated this process until the multivariate model R^2 could no longer be improved by >0.02 by adding a single variable.

With many potential predictors, there is a substantial risk of overfitting a multivariate model. To reduce this risk, we used cross-validation to evaluate the true predictive power of each of the 1,097 growth models. Cross-validation involves sequentially removing one RWI value at a time, calculating new regression coefficients using the climate and ring-width data from all other years, and predicting the missing RWI value. The correlation coefficient yielded by correlating these modeled RWI values with actual values is more representative of each model's true predictive power because each modeled RWI value was calculated using a model developed using independent data (24).

Cross-validated correlation of modeled and actual RWI records produced a significance of $P < 0.01$ for 963 of the 1,097 (88%) records evaluated. However, a P value of 0.01 underestimates the true probability of a false statistical relationship between modeled and actual ring widths because each growth model had more than one opportunity to include a false but statistically present relationship. We therefore limited all projections of 21st century growth to the 853 sites where modeled and actual RWI values correlated with a cross-validated P value of <0.001 . Although significance tests (P values) are not technically valid for cross-validated correlations, we felt that using such a strict standard for model acceptability sufficiently minimized our risk of using growth models that assumed false relationships between growth and climate.

Importantly, climate can affect tree growth over more than just one growing season. Physiological and stand-dynamics effects that are not related to climate can also affect growth over multiple consecutive growing seasons. These multiyear effects on tree growth often cause autocorrelation within RWI records. To isolate only year-to-year variability in the ring-width record, this autoregressive component is often removed before analysis in tree-ring studies (25). After extensive testing, however, we determined that removing the autoregressive component from ring-width records did not result in a substantial improvement to the accuracy of most ring-width models. In fact, many models performed substantially worse on these "pre-whitened" ring-width records.

Climate also impacts tree growth in a nonlinear fashion. For example, additional precipitation may only contribute to continued growth until the soil is saturated. Growth models often account for issues such as above-ground runoff and hygrostatic soil properties using a soil water balance term that accounts for how precipitation rate, temperature, humidity, soil properties, and conductive properties of overlying vegetation interact to impact water availability to plants (26–28). We did not use such a variable in this study, however, because we did not know enough about the soil or plant properties at each site to make accurate calculations of soil-water balance.

An alternate method of dealing with nonlinear relationships between climate and ring width was to simply include nonlinear growth predictors into the growth models. In an analysis where models were allowed to include quadratic relationships, nonlinear relationships with precipitation were most commonly chosen at sites throughout the Rocky Mountains. Nonlinear relationships with temperature were most common in the northwestern US. However, there was no obvious commonality among sites and/or

species within these regions where nonlinear relationships substantially improved model performance. Therefore, it seemed likely that the addition of a nonlinear component to the model-building process would lead to overfitting of many ring-width models, and we ultimately did not allow for the incorporation of nonlinear relationships in any of the ring-width models.

Growth response to 21st century climate. We used the PRISM climate dataset to model RWI values at each site from 1950 to 1999. We then used four distinct scenarios of 21st century climate to model 2050–2099 RWI values. For each scenario, we compared the average modeled 1950–1999 RWI value to that for 2050–2099 and then calculated the percent change in annual growth rate due to climate change (cf. ref. 29).

The datasets representing the first two scenarios were developed by the National Center for Atmospheric Research (NCAR) using the CCSM3 General Circulation Model (GCM). We obtained these datasets from the World Climate Research Program's (WCRP's) Coupled Model Intercomparison Project phase 3 (CMIP3) multimodel dataset. The first scenario represents the A2 case, which assumes business-as-usual greenhouse gas emissions throughout the 21st century (30). The second scenario represents the A1B case, which assumes that the rate of greenhouse gas accumulation in the atmosphere will slow after 2050 (31). These model datasets are gridded, with 1.4-degree spatial resolution, and are identical from 1896 through 1999.

We downscaled the 1.4-degree CCSM3 climate projections so that they matched the 1896–1999 mean and variability at each tree-ring site. To do this, we first upscaled the original 2.5 arc-minute PRISM data to 1.4-degree spatial resolution and adjusted the CCSM3 modeled datasets so that their means from 1896 to 1999 matched those of the upscaled PRISM datasets. We then determined the linear relationship between the 1.4-degree PRISM data and the site-specific (3 by 3 grid around each tree-ring site) PRISM data using linear regression. Finally, we used this relationship between site-specific and 1.4-degree PRISM climate data to downscale the already adjusted CCSM3 modeled climate data to represent each site.

The third and fourth 21st century climate scenarios did not use low-resolution climate data generated by a GCM. They assumed that linear climate trends already established during previous decades will continue throughout the 21st century. The third scenario assumed that any linear climate trends established in the PRISM dataset from 1895 through 2008 will continue through 2099. The fourth scenario only considered linear trends established from 1979 through 2008, when observed warming accelerated globally. For each tree-ring record, we created annual climate projections for 2009 through 2099 by shifting the values from 1909 to 1999 according to the appropriate linear trend. In the cases of very strong trends in these third and fourth scenarios, we did not allow extrapolated precipitation to become negative and we confined extrapolated relative humidity values to between zero and 100%.

The use of prestandardized ring-width index records. An unavoidable drawback to using records of tree-ring widths to establish relationships between tree growth and climate variability is that there are trends in records of tree-ring widths that are caused by nonclimate factors. These trends generally occur over the course of decades to centuries and, because they are not associated with climate, they must be statistically removed from the ring-width records before associations between ring widths and climate can be accurately quantified (12, 22).

The standardization process is partly subjective but usually implemented systematically. Careful consideration of individual tree-ring series is often required to determine the appropriate standardization technique, and although some series may be detrended by specifically choosing curve types, most series within sites are based on a common curve fitting approach. The most common trend that is removed is a negative exponential-type trend

of declining ring widths caused by the ever-increasing cross-sectional area of the trunk of a growing tree. Also common is a temporary trend toward increasing ring widths during the beginning years or decades of a tree's life as its roots become increasingly established and growth allocation gradually shifts from height to girth (32). Changes in ring widths may also be removed if they are believed to be caused by stand dynamics that are not directly related to climate variability. For example, ring widths may be temporarily suppressed due to broken branches caused by a fallen neighboring tree or ring widths may become wider due to reduced competition after the death or removal of a neighboring tree. These effects may be indicated by unique growth changes within just one or a few trees rather than the whole set of trees sampled in a site.

Without substantial care, however, standardization can easily counteract its purpose by introducing false trends in ring-width records. The ends of ring-width records are particularly vulnerable to these effects (33). For example, the removal of a linear trend from a record that decreases somewhat logarithmically causes an artificial increase in ring-width index values at the end of the record. On the other hand, removal of a negative exponential trend from a record that decreases linearly causes an artificial decrease in ring-width index values at the end of the record. To avoid artifacts of standardization, it is fairly common to apply a smoothing spline to remove all low-frequency variability that occurs beyond some temporal threshold. This type of trend removal must be done with care, however, because it does not discriminate between low-frequency variability caused by nonclimate processes and those caused by relatively slow climate processes such as the Pacific Decadal Oscillation, Medieval Warm Period, and Little Ice Age.

A shortcoming intrinsic to all standardization techniques is that relationships between tree growth and climate variability on decadal to centennial scales are often removed. This means that, to some degree, standardized ring-width index records do not fully reflect trees' ability to acclimate to long-term trends in environmental conditions. Such acclimations are known to occur and have been observed as reallocations of resources among various parts of the tree (7). In an attempt to identify long-term growth trends in forests across western North America, McKenzie et al. (21) performed very conservative standardizations to remove ring-width trends caused by tree size and keep as much low-frequency variability in ring widths as possible. The goal of that study was to identify tree populations that may have experienced increased radial growth in recent decades, so the conservative standardization techniques used were meant to safely error on the side of retaining negative growth trends associated with tree size. This gave the authors confidence that the few populations that showed positive poststandardized ring-width trends truly did experience a positive growth trend.

To error on the side of understandardization, however, is to introduce false statistical relationships between RWI values and climate. Thus, we chose to use the prestandardized ring-width index records provided by the ITRDB because they were presumably standardized by individuals who carefully considered how to best standardize each individual ring-width record using a certain amount of expertise on the site and the sampled population. We felt that although it may appear to be more scientifically sound to start with raw ring-width records and standardize all records using a consistent and conservative technique, an automated standardization process would likely cause more problems than it would solve, particularly by introducing artificial trends to the ends of ring-width index records that could easily be misinterpreted as responses to 20th century climate change.

To evaluate the impact of standardization on the relationships between the RWI records used in this study and low-frequency climate variability, we tested how well modeled and actual RWI records correlate after both records undergo varying degrees of

smoothing. The theory is that modeled RWI records reflect the climate processes that occurred across a broad range of time scales but actual RWI records do not. For example, if a ring-width record is standardized by removing the 45-y running mean, then the resultant RWI record can only reflect climate processes that occurred on time scales shorter than 45 y. Therefore, modeled and actual RWI records smoothed with, say, a 5-y running mean should correlate fairly well, but modeled and actual RWI records smoothed with a 51-y running mean should not correlate well because the modeled record would still reflect low-frequency climate variability while the actual record would consist only of values very close to 1.

Fig. S2 indicates that for the vast majority of the 853 RWI records with well-performing models within the continental US, correlations between modeled and measured RWI records remained strong when running means were calculated with windows as wide as 50–60 y. For SW populations, correlations between running-mean modeled and actual RWI records tended to be stronger, but they also tended to decrease substantially when running means were calculated using 50- to 60-y windows. These results indicate that RWI records generally represent climate variability on time scales of a half century and shorter. This is particularly true among RWI records from the SW US.

This analysis indicates that the majority of SW ring-width records have been standardized in a relatively conservative manner that preserves multidecadal variability in interannual growth rates. Although anthropogenic climate change is certainly expected to occur on time scales longer than several decades, the accurate representation of growth response to climate processes on time scales out to 50 y and often beyond indicates that if low-frequency climate variability causes trees to begin using adaptation strategies within 50 y or so, then those adaptation processes are likely reflected in many of the growth equations for tree populations in the SW US.

Methods of Wildfire and Bark-Beetle Analysis. In September 2009, we obtained annual shapefiles of insect-induced forest mortality for Arizona, New Mexico, Utah, and Colorado from the US Forest Service (USFS) Forest Health Technology Enterprise Team (FHTET, www.fs.fed.us/foresthealth/technology/ads_standards.shtml). This dataset represented years 1997 through 2008. We constrained our analysis to tree mortality attributed to bark-beetle infestation because it is likely that warming and drought stress within a forest both contribute to increasing the probability of bark-beetle infestation (34–36). We also obtained fire-burn severity data for all wildfires within the SW US from 1984 to 2006 from the US government's Monitoring Trends in Burn Severity project (MTBS, www.mtbs.gov). For each year, we calculated the percent of SW forest and piñon-juniper woodland area that was reported to have been affected by each of these mortality processes.

For bark-beetle-induced mortality, FHTET identified regions where >50% of trees had been killed. For fire-induced mortality, there is no calibrated measure of the percent of trees killed. Instead, MTBS classifies burned pixels as “low,” “moderate,” and “severe.” We inferred that “moderate” and “severe” classifications within forest or piñon-juniper woodland areas indicate that there was substantial tree mortality. The detailed methodology that MTBS follows to classify burn severity is described in Key and Benson (37). In short, burn severity classifications were based on the total change in the Normalized Burn Ratio (NBR) during the peak of the growing season before and after burn events. NBR is based on the difference between near-infrared (0.76–0.90 μm) and middle-infrared (2.08–2.35 μm) surface reflectance, similar to the popularly used normalized difference vegetation index (NDVI). High reflectance in the near-infrared is associated with low chlorophyll content. Low reflectance in the middle-infrared has been shown to be associated with low water content and high amounts of soil, ash, and charred wood (38). So, subtracting the postburn NBR from the preburn NBR results in

a positive value (dNBR). The more positive the dNBR, the more severe the fire is assumed to have been. Notably, basing burn severity classifications upon the total difference in NBR between images leads to a bias toward low-burn severity classifications in areas with low vegetation densities such as piñon-juniper woodland. Although much of the existing vegetation in a sparsely populated area may be thoroughly burned, the average near- and middle-infrared reflectance across a 30-m pixel will not result in as high of a change in NBR values as they would in a more densely populated stand of trees. For this reason, a relativized version of the dNBR (RdNBR) has been developed (39–41). However, generalized rules for burn-severity classification using the RdNBR have not yet been established and applied to the long-term wildfire record used in this study. Therefore, our estimates of forest and woodland area experiencing “moderate” and “severe” wildfire burns are very likely conservative underestimates.

To calculate the percent of forest and piñon-juniper woodland affected by substantial tree mortality, we first estimated the distribution and total area of SW forest and piñon-juniper woodland before 1984 (the first year of the burn-severity analysis). To do this, we used three datasets of land cover. The datasets were the 1981 Brown and Lowe classification of biotic communities in the SW US (42), the 1992 National Land Cover Data Set (NLCD, <http://landcover.usgs.gov>), and the 2004 Southwest Regional Landcover Data (ReGAP, <http://earth.gis.usu.edu/swgap/landcover.html>). We accessed each of these datasets in September 2009. The NLCD and ReGAP datasets have 30-m spatial resolution. The Brown and Lowe dataset is a set of geographic polygons (ArcGIS shapefile) with relatively coarse spatial resolution (1:1,000,000). We resampled this dataset to convert it to a grid of 30-m pixels.

We originally considered forested areas to be areas classified by Brown and Lowe as any kind of conifer forest. We considered piñon-juniper woodland areas to be areas classified by Brown and Lowe as “Great Basin conifer woodland” or “Madrean evergreen woodland.” However, the coarse spatial resolution of the Brown and Lowe dataset causes inaccuracies in the locations of the boundaries between land-cover types. For example, areas identified as woodland in the Brown and Lowe analysis were often classified as conifer forest in the NLCD and ReGAP datasets. We therefore incorporated the higher resolution NLCD, making the assumption that, in general, anything classified as “evergreen forest” or “mixed forest” in the 1992 NLCD was probably the same in 1981. In other words, we considered forest to be present in all locations classified as forest by either Brown and Lowe or 1992 NLCD. We could not make this same assumption for piñon-juniper woodland because the 1992 NLCD does not distinguish between piñon-juniper woodland and other types of nontree shrubland. However, the 2004 ReGAP analysis does make this distinction. We therefore considered piñon-juniper woodland to be present at any nonforest location identified as “Great Basin conifer woodland” or “Madrean evergreen woodland” by Brown and Lowe and/or as both “woodland” by the 1992 NLCD and “piñon-juniper woodland” by the 2004 ReGAP. Finally, we also made the assumption that all areas field-mapped as displaying bark-beetle mortality since 1997 must be either forest or piñon-juniper woodland. There were 647 km² affected by beetle-induced tree mortality which were not classified as forest or piñon-juniper woodland using the classification method described above. We classified these zones as piñon-juniper woodland because the vast majority of these zones were near the low-elevation piñon-juniper ecotone. Because we incorporated the Brown and Lowe classification, which only extends to 37.5 °N, the SW region evaluated in the mortality analysis was 8% smaller (55,501 km²) than the SW region considered in the tree-ring analysis, which extends to 38 °N.

Certainly, given this rather complicated land-cover classification scheme, there are errors associated with our estimates of the area of forest and woodland affected by fire- and beetle-induced tree mortality. To evaluate the possible magnitude and range of

these errors, we repeated the annual analysis using five different methods to define forest and piñon-juniper woodland. These five methods were as follows:

Method 1.

Forest.

- i. Any area defined by Brown and Lowe as conifer forest.
- ii. Any area defined by 1992 NLCD as evergreen or mixed forest.

Piñon-juniper woodland.

- i. Any nonforest area defined by Brown and Lowe as Great Basin conifer woodland or Madrean evergreen woodland.
- ii. Any nonforest area defined by 1992 NLCD as woodland and by 2004 ReGAP as piñon-juniper woodland.
- iii. Any area affected by bark-beetle tree mortality but not found to be forest or piñon-juniper woodland using the above methods.

Method 2.

Forest.

- i. Same as in Method 1.

Piñon-juniper woodland.

- i. Same as in Method 1, except not including piñon-juniper woodland areas defined in (iii) above.

Method 3.

Forest.

- i. Any area defined by Brown and Lowe as conifer forest.

Piñon-juniper woodland.

- i. Any area defined by Brown and Lowe as Great Basin conifer woodland or Madrean evergreen woodland.

Method 4.

Forest.

- i. Any area defined by 1992 NLCD as evergreen or mixed forest.

Piñon-juniper woodland.

- i. Any nonforest area defined by 1992 NLCD as woodland and by 2004 ReGAP as piñon-juniper woodland.
- ii. Any area affected by bark-beetle tree mortality but not found to be forest or piñon-juniper woodland using the above methods.

Method 5.

Forest.

- i. Same as in Method 4.

Piñon-juniper woodland.

- i. Same as in Method 4, except not including piñon-juniper woodland areas defined in (ii) above.

Among these five methods, method 2 produced the lowest estimate of percent forest and piñon-juniper woodland affected by 1997–2008 beetle-induced tree mortality and method 4 produced the highest (7.33% and 11.31%, respectively). Importantly, four of the five methods produced estimates between 7.33% and 9.06%. For 1984–2006 wildfire-induced mortality, method 2 produced the lowest estimate (2.68%) and method 5 produced the highest (3.07%). Table S2 lists how each method impacted the overall size of the SW region considered, the total areas of forest and piñon-juniper woodland, and the amount of each of these land-cover types mapped as affected by tree mortality associated with bark beetles from 1997 to 2008 and wildfire burns from 1984 to 2006.

Although estimates of total area of forest and piñon-juniper woodland affected by these mortality agents varied according to the methods used to define vegetation type, the annual calculations were impressively consistent among the five methods (Fig. S3). This was also generally the case when forest and piñon-juniper woodland areas were considered independently. As an exception, there was substantial variability among annual records of piñon-juniper woodland affected by fire-induced mortality. The percent area of piñon-juniper woodland affected by fire was very small compared with the percent forest area affected by fire, however. Therefore, disagreement among estimates of piñon-juniper area burned did not result in large differences in estimates of overall forest and piñon-juniper area affected by fire-induced tree mortality.

Notably, these estimates of area experiencing substantial tree mortality due to fire are probably too low because of the bias inherent in the dNBR calculation, described in the second paragraph of this section. To evaluate the degree to which this bias may impact our calculations, we included “low” burn areas and recalculated annual and total percentages of forest and piñon-juniper woodland area that experienced tree mortality due to fire. We made these calculations using method 1 (described above) and duplicated them with method 4 to again test the impact of our uncertainty in the pre-1984 spatial distribution of forest and piñon-juniper woodland. The two methods resulted in generally similar annual calculations (Fig. S5). By including low burn areas in the fire-induced mortality analysis, the overall area of forest and piñon-juniper woodland affected increased by 72% using method 1 (method 4: 75%). Although high amounts of tree mortality certainly did not occur in all low burn areas, including all low burn areas offers an estimate of the absolute highest possible error that could have occurred because of the dNBR bias.

For forest area only, including low burn areas increased estimates of forested area affected by fire-induced mortality by 68% (method 4: 70%). For piñon-juniper woodland, the area increased by 95% (method 4: 106%). Given that the bias toward lower burn severity is strongest in areas with low tree density, it is likely that the underestimation of mortality due to “moderate” and “severe” burns was larger for piñon-juniper woodland than it was for forest. However, this impact of this error in piñon-juniper woodland probably has only a small impact on the estimates of overall forest and piñon-juniper area that experienced mortality due to fire because the overall burned area of piñon-juniper woodland is relatively low. As an example, the overall area of fire-induced mortality within SW forest and woodland would only increase from 2.68% to 3.21% if low severity burns in woodland were considered to lead to widespread mortality (method 4: 3.03% to 3.36%).

Fig. S5 demonstrates that the annual percent of area burned within each vegetation type increased for all three burn severity classes from 1984 through 2006. As the annual burned area tended to increase over time, the annual percentage of forest and piñon-juniper woodland area burned at low severity increased faster than the percentage of the more severe burn types.

Viewed in another way, interesting trends emerge. Although burned area increased from 1984 to 2006 among all three severity classifications, Fig. S6 indicates a shift toward a greater proportion of severe fires within forests and a greater proportion of low and moderate severity fires in piñon-juniper woodland. The reason for this is not immediately clear and warrants further investigation.

1. Allen CD, Breshears DD (1998) Drought-induced shift of a forest-woodland ecotone: Rapid landscape response to climate variation. *Proc Natl Acad Sci USA* 95:14839–14842.
2. Breshears DD, et al. (2005) Regional vegetation die-off in response to global-change-type drought. *Proc Natl Acad Sci USA* 102:15144–15148.
3. Swetnam TW, Betancourt JL (1998) Mesoscale disturbance and ecological response to decadal climatic variability in the American Southwest. *J Clim* 11:3128–3147.
4. Allen CD, et al. (2010) A global overview of drought and heat-induced tree mortality reveals emerging climate change risks for forests. *Forest Ecol Manag* 259:660–684.

5. van Mantgem PJ, et al. (2009) Widespread increase of tree mortality rates in the western United States. *Science* 323:521–524.
6. Hicke JA, et al. (2002) Trends in North American net primary productivity derived from satellite observations, 1982–1998. *Global Biogeochem Cycles* 16:1018.
7. Lapenis A, Shvidenko A, Shepaschenko D, Nilsson S, Ayyer A (2005) Acclimation of Russian forests to recent changes in climate. *Glob Change Biol* 11:2090–2102.
8. Running SW, et al. (2004) A continuous satellite-derived measure of global terrestrial primary production. *Bioscience* 54:547–560.

9. Phillips OL, et al. (2009) Drought sensitivity of the Amazon rainforest. *Science* 323: 1344–1347.
10. Saleska SR, Didan K, Huete AR, da Rocha HR (2007) Amazon forests green-up during 2005 drought. *Science* 318:612.
11. Samanta A, et al. (2010) Amazon forests did not green up during the 2005 drought. *Geophys Res Lett* 37:L05401.
12. Fritts HC (1976) *Tree Rings and Climate* (Academic, New York).
13. Hughes MK, Swetnam TW, Diaz H (2010) *Developments in Paleoenvironmental Research*, ed. Smol JP (Springer, New York). Vol. 11, pp 340.
14. Biondi F (1999) Comparing tree-ring chronologies and repeated timber inventories as forest monitoring tools. *Ecol Appl* 9:216–227.
15. Thammincha S (1981) Climatic variation in radial growth of Scots pine and Norway spruce and its importance in growth estimation. *Acta Forestalia Fennica* 171:1–57.
16. Ettl GJ, Peterson DL (1995) Growth response of subalpine fir (*Abies lasiocarpa*) to climate in the Olympic Mountains Washington, USA. *Glob Change Biol* 1:213–230.
17. Holman ML, Peterson DL (2006) Spatial and temporal variability in forest growth in the Olympic Mountains, Washington: Sensitivity to climatic variability. *Can J For Res* 36:92–104.
18. Nakawatase JM, Peterson DL (2006) Spatial variability in forest growth—climate relationships in the Olympic Mountains, Washington. *Can J For Res* 36:77–91.
19. Peterson DW, Peterson DL (2001) Mountain hemlock growth responds to climatic variability at annual and decadal time scales. *Ecology* 82:3330–3345.
20. Peterson DW, Peterson DL, Ettl GJ (2002) Growth responses of subalpine fir to climatic variability in the Pacific Northwest. *Can J For Res* 32:1503–1517.
21. McKenzie D, Hessl AE, Peterson DL (2001) Recent growth of conifer species of western North America: Assessing spatial patterns of radial growth trends. *Can J For Res* 31: 526–538.
22. Cook ER, Briffa K, Shiyatov S, Mazepa V (1990) *Methods of Dendrochronology: Applications in the Environmental Sciences*, eds Cook ER, Kairiukstis LA (Kluwer Academic Publishers, Boston), pp 104–123.
23. Ward JK, Strain BR (1999) Elevated CO₂ studies: Past, present and future. *Tree Physiol* 19:211–220.
24. Michaelsen J (1987) Cross-validation in statistical climate forecast models. *J Clim Appl Meteorol* 26:1589–1600.
25. Meko D, Graybill DA (1995) Tree-ring reconstruction of upper Gila River Discharge. *Water Resour Bull* 31:605–616.
26. Stephenson NL (1990) Climatic control of vegetation distribution: The role of the water balance. *Am Nat* 135:649–670.
27. Stephenson NL (1998) Actual evapotranspiration and deficit: Biologically meaningful correlates of vegetation distribution across spatial scales. *J Biogeogr* 25:855–870.
28. Williams AP, Still CJ, Fischer DT, Leavitt SW (2008) The influence of summertime fog and overcast clouds on the growth of a coastal Californian pine: A tree-ring study. *Oecologia* 156:601–611.
29. Grissino-Mayer HD, Fritts HC (1995) *Storm over a Mountain Island: Conservation Biology and the Mount Graham Affair*, eds Hoffman R, Istock C (Univ Arizona Press, Tucson), pp 100–120.
30. Thomas CD, et al. (2004) Extinction risk from climate change. *Nature* 427:145–148.
31. IPCC (2007) *Synthesis Report. Contribution of Working Groups I, II and III to the Fourth Assessment Report of the Intergovernmental Panel on Climate Change* (Cambridge Univ Press, Cambridge, UK).
32. Warren WG (1980) On removing the growth trend from dendrochronological data. *Tree-Ring Bulletin* 40:35–44.
33. Cook ER, Briffa KR, Meko DM, Graybill DA, Funkhouser G (1995) The 'segment length curse' in long tree-ring chronology development for palaeoclimatic studies. *Holocene* 5:229–237.
34. Bentz B, et al. (2009) *Bark Beetle Outbreaks in Western North America: Causes and Consequences* (Univ Utah Press, Salt Lake City).
35. Logan JA, Régnière J, Powell JA (2003) Assessing the impacts of global warming on forest pest dynamics. *Front Ecol Environ* 1:130–137.
36. Raffa KF, et al. (2008) Cross-scale drivers of natural disturbances prone to anthropogenic amplification: The dynamics of bark beetle eruptions. *Bioscience* 58:501–517.
37. Key CH, Benson NC (2005) in *FIREMON: Fire Effects Monitoring and Inventory System. General Technical Report RMRS-GTR-164-CD: LA1-LA51* (US Dept Agric, Rocky Mt Res Sn, Ogden, UT).
38. Jia GJ, Burke IC, Goetz AFH, Kaufmann MR, Kindel BC (2006) Assessing spatial patterns of forest fuel using AVIRIS data. *Remote Sens Environ* 102:318–327.
39. Holden ZA, Morgan P, Evans JS (2009) A predictive model of burn severity based on 20-year satellite-inferred burn severity data in a large southwestern US wilderness area. *For Ecol Manage* 258:2399–2406.
40. Miller JD, et al. (2009) Calibration and validation of the relative differenced Normalized Burn Ratio (RdNBR) to three measures of fire severity in the Sierra Nevada and Klamath Mountains, California, USA. *Remote Sens Environ* 113:645–656.
41. Miller JD, Thode AE (2007) Quantifying burn severity in a heterogeneous landscape with a relative version of the delta Normalized Burn Ratio (dNBR). *Remote Sens Environ* 109:66–80.
42. Brown DE (1982) Biotic communities of the American Southwest: United States and Mexico [Western States (USA); Great Basin and Pacific Slope States]. *Desert Plants* 4:1–342.

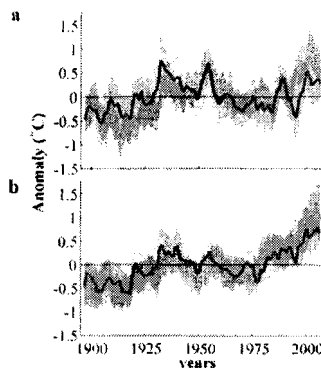


Fig. S1. Running 5-year average departure from mean daily maximum temperature (A) and minimum temperature (B) anomaly in the southwestern region highlighted in Fig. 1 (orange area and red line) and the rest of the continental United States (gray area and gray line). Thick lines represent the median PRISM pixel value within the region. Shaded areas represent the inner quartiles of pixel values (50% of pixel values lie within the shaded region).

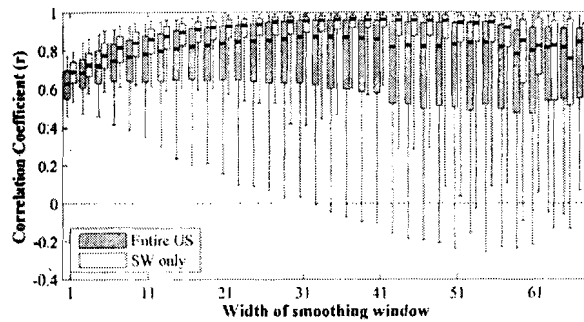


Fig. S2. Box plots of correlation coefficients calculated by comparing smoothed time series of modeled RWI values to smoothed time series of actual RWI values. Smoothing was done using running means across various window lengths ranging from 1 to 67 y. All correlations used at least 35 y of smoothed data. We only considered the 853 models used in our main analysis. Boxes bound inner quartiles. Whiskers bound the inner 90% of values. Thick black lines represent median values.

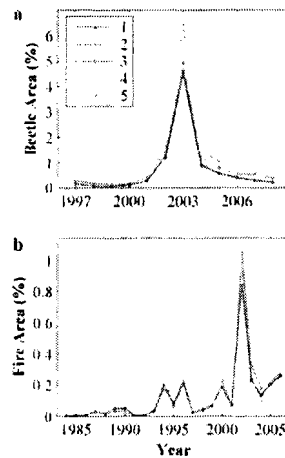


Fig. S3. Annual percent of forest and piñon-juniper area impacted by mortality caused by bark beetles (A) and moderate and severe wildfire burns (B) for each of the five methods used to define forest and piñon-juniper woodland. The five methods are described in *SI Text: Methods for Wild Fire and Bark-Beetle Analysis*. Method 1 was used in our final analysis.

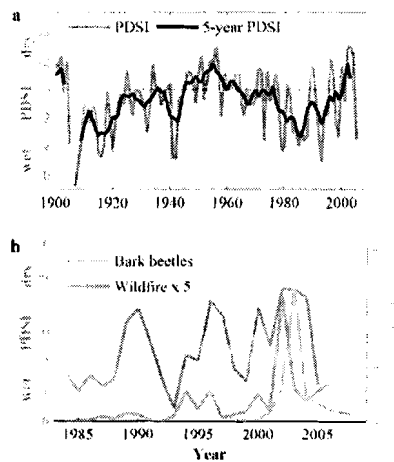


Fig. S4. (A) Annual mean and 5-y running mean Palmer Drought Severity Index (PDSI). Annual PDSI was calculated as mean monthly October–September in the SW region. PDSI data are gridded spatially at 2.5-degree spatial resolution (1). (B) Annual percent of forest and piñon-juniper area impacted by mortality caused by bark beetles (orange) and moderate and severe wildfire burns (red) overlaid on annual PDSI. Note that the wildfire burn area is multiplied by 5 here for visualization.

1. Dai A, Trenberth KE, Qian T (2004) A global dataset of Palmer Drought Severity Index for 1870–2002: Relationship with soil moisture and effects of surface warming. *J Hydrometeorol* 5: 1117–1130.

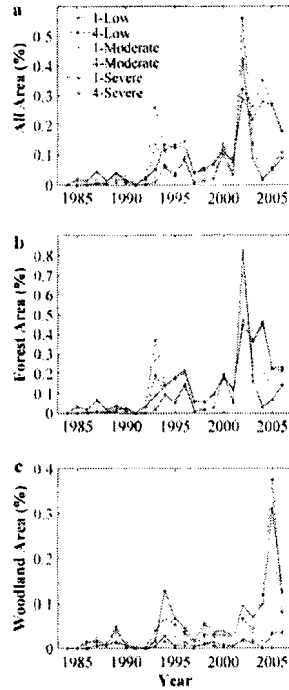


Fig. 55. Annual percent of forest and piñon-juniper woodland (A), forest only (B), and piñon-juniper woodland (C) only burned by low (blue), moderate (orange), severe (brick red) fire. Solid lines and dashed lines represent time series calculated using methods 1 and 4, respectively. These methods are described in *SI Text: Methods for Wild Fire and Bark-Beetle Analysis*.

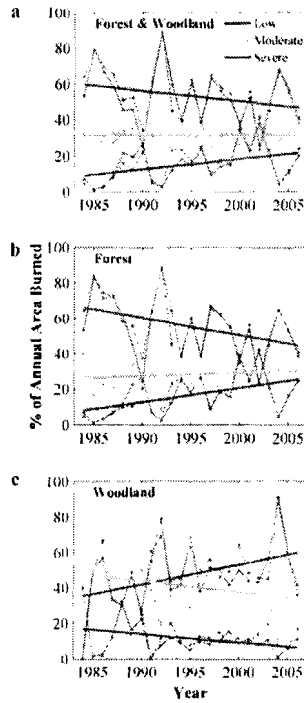


Fig. 56. The percent of annual area burned classified as low (blue), moderate (orange), and severe (brick red) within forest and piñon-juniper woodland (A), forest only (B), and piñon-juniper woodland only (C). Thin solid lines and dashed lines represent time series calculated using methods 1 and 4, respectively. Thick lines follow linear annual trends for method 1 calculations. Methods 1 and 4 are described in *SI Text: Methods for Wild Fire and Bark-Beetle Analysis*.

Table S1. Projected changes in 50-y mean RWI values for the 235 chronologies from the SW region, comparing 2050–2099 to 1950–1999

Species	Scenario	Δ RWI, %			
		Mean	Median	Upper 25%	Lower 25%
PIED	A2	-40	-38	-15	-62
	A1B	-27	-24	-8	-47
	114-y	-11	-4	4	-27
	30-y	-140	-104	-78	-164
PIPO	A2	-48	-48	-15	-72
	A1B	-34	-34	-5	-28
	114-y	-17	-11	5	-28
	30-y	-123	-99	-45	-171
PSME	A2	-48	-43	-23	-63
	A1B	-35	-32	-15	-50
	114-y	-14	-11	0	-24
	30-y	-119	-111	-63	-161

PIED, piñon pine; PIPO, ponderosa pine, PSME, Douglas fir.

Table S2. SW Area (km²) impacted by tree mortality due to wildfires from 1984 to 2006 and bark beetles from 1997 to 2008

		Method				
		1	2	3	4	5
SW Area	Overall SW area	664,839	664,839	664,839	720,392	720,392
	Area of Forest	123,395	123,395	60,811	122,350	122,350
	Area of Woodland	116,443	115,796	147,154	59,933	55,424
	Area of Forest or Woodland	239,838	239,191	207,965	182,283	177,774
	% Forest	18.56	18.56	9.15	16.98	16.98
	% Woodland	17.51	17.42	22.13	8.32	7.69
Bark beetles	Total Area	18,177	18,177	18,177	20,619	20,619
	Area of Forest	13,251	13,251	7,899	13,542	13,542
	Area of Woodland	4,926	4,279	8,616	7,078	2,568
	Area of Forest or Woodland	18,177	17,530	16,515	20,619	16,110
	% Forest	10.74	10.74	12.99	11.07	11.07
	% Woodland	4.23	3.70	5.86	11.81	4.63
Wildfire	% Forest or Woodland	7.58	7.33	7.94	11.31	9.06
	Total Area	9,596	9,596	9,596	9,965	9,965
	Area of Forest	5,076	5,076	3,326	4,963	4,963
	Area of Woodland	1,344	1,336	2,270	566	489
	Area of Forest or Woodland	6,420	6,412	5,596	5,528	5,452
	% Forest	4.11	4.11	5.47	4.06	4.06
Wildfire or beetle	% Woodland	1.15	1.15	1.54	0.94	0.88
	% Forest or Woodland	2.68	2.68	2.69	3.03	3.07
	Total Area	27,288	27,288	27,287	30,080	30,080
	Area of Forest	17,844	17,844	10,882	18,015	18,015
	Area of Woodland	6,245	5,598	10,777	7,588	3,049
	Area of Forest or Woodland	24,089	23,442	21,659	25,604	21,065
	% Forest	14.46	14.46	17.89	14.46	14.46
	% Woodland	5.36	4.83	7.32	4.83	5.36
	% Forest or Woodland	10.04	9.80	10.41	9.80	10.04

The five columns represent unique methods of defining forest, woodland, and the SW US. These methods are described in *SI Text* on "Methods of Wildfire and Bark-Beetle Analysis." The main text reports the results of method 1.